Pergamon

www.neuroscience-ibro.com

PII: S0306-4522(02)00512-2

Neuroscience Vol. 115, No. 2, pp. 587–602, 2002

0306-4522/02 $22.00+0.00

LOSS OF CARDIOLIPIN AND MITOCHONDRIA DURING PROGRAMMED NEURONAL DEATH: EVIDENCE OF A ROLE FOR LIPID PEROXIDATION AND AUTOPHAGY

R. A. KIRKLAND, R. M. ADIBHATLA, J. F. HATCHER and J. L. FRANKLIN*

Department of Neurological Surgery, University of Wisconsin Medical School, 4640 MSC, 1300 University Avenue, Madison, WI 53706, USA

Abstract—Cardiolipin, a lipid of the mitochondrial inner membrane, is lost from many types of cells during apoptotic death. Here we show that the cardiolipin content of nerve growth factor (NGF)-deprived rat sympathetic neurons undergoing apoptotic death in cell culture decreased before extensive loss of mitochondria from the cells. By 18–24 h after NGF deprivation, many neurons did not stain with the cardiolipin-specific dye, Nonyl Acridine Orange, suggesting complete loss of cardiolipin. Gas chromatography confirmed the decline of cardiolipin content in NGF-deprived neurons. Electron microscopy and immunoblots for the mitochondrial-specific protein, heat shock protein 60 (HSP60), revealed that there was only a slight decrease in mitochondrial mass at this time. Cardiolipin loss after NGF deprivation was concurrent with increased production of mitochondrial-derived reactive oxygen species [Kirkland, R.A., Franklin, J.L., 2001. J. Neurosci. 21, 1949–1963] and increased lipid peroxidation. Compounds having antioxidant effects blocked peroxidation, loss of cardiolipin, and the decrease of mitochondrial mass in NGF-deprived neurons. These compounds also blocked an increase in the number of lysosomes and autophagosomes in NGF-deprived cells.

The findings reported here show that the important mitochondrial inner membrane lipid, cardiolipin, is lost from mitochondria during neuronal apoptosis and that this loss occurs before significant loss of mitochondria from cells. They suggest that the loss of cardiolipin is mediated by free radical oxygen.

Key words: apoptosis, reactive oxygen, free radical, cytochrome *c*, cell death, Nonyl Acridine Orange.

Approximately half of the neurons produced during the development of the vertebrate nervous system undergo apoptotic death (Oppenheim, 1991; Pettman and Henderson, 1998). A major factor influencing which cells survive the period of developmental apoptosis is the availability of a sufficient quantity of a required neurotrophic factor, such as nerve growth factor (NGF). The classic model system used to investigate the cellular and molecular events underlying apoptosis during neurogenesis consists of NGF-deprived embryonic rat or mouse sympathetic neurons in cell culture (Martin et al., 1988; Deckwerth and Johnson, 1993; Deshmukh et al., 1996; Kirkland and Franklin, 2001). Like many other cell types undergoing apoptosis, NGF-deprived sympathetic neurons release cytochrome *c* from the mitochondrial intermembrane space into the cytoplasm where it then binds onto the caspase regulatory protein, apoptosis protease activating factor-1, and triggers caspase activity (Kluck et al., 1997; Li et al., 1997; Reed, 1997; Zou et al., 1997; Deshmukh and Johnson, 1998; Martinou et al., 1999). The activated caspases in turn cleave many important protein substrates, causing cellular demise.

The pathway(s) by which cytochrome *c* exits mitochondria during apoptosis is unclear. One proposed escape route is mechanical disruption of the mitochondrial outer membrane (OM) induced by swelling of the mitochondrial matrix (Lemasters et al., 1998; Von Ahsen et al., 2000). While this mechanism seems important in some cell types, it is clear that this cannot be the means of exit in NGF-deprived sympathetic neurons, as the mitochondria in these cells show little obvious morphological change during the period of cytochrome *c* redistribution (Martinou et al., 1999). Here we report, while there is negligible alteration in the morphology of individual mitochondria during this time, that mitochondria, nevertheless, appear to sustain damage. We recently demonstrated that elevated levels of mitochondrial-derived reactive oxygen species (ROS) occur in NGF-deprived sympathetic neurons during the period of cytochrome *c* release. These ROS are attenuated by pan-caspase inhibitors and blocked by compounds that increase cellular glutathione concentration (Kirkland and Franklin, 2001). These findings suggest that caspase

*Corresponding author. Tel.: +1-608-263-5468; fax: +1-608-265-3461.

E-mail address: jlfrankl@facstaff.wisc.edu (J. L. Franklin).

Abbreviations: ANOVA, analysis of variance; BAF, boc-aspartyl(OMe)-fluoromethylketone; CHX, cycloheximide; $DiIC_{18}$, 1,1′-dioctadecyl-3,3,3′,3′-tetramethylindocarbocyanine perchlorate; EM, electron microscopy; FCCP, carbonyl cyanide *p*-trifluoromethoxyphenylhydrazone; HSP60, heat shock protein 60; IM, inner membrane; L-NAC, *N*-acetyl-L-cysteine; NAO, Nonyl Acridine Orange; NGF, nerve growth factor; OM, outer membrane; ROS, reactive oxygen species; TBS, Tris-buffered saline.

activity, initiated by cytoplasmic cytochrome *c*, augments mitochondrial ROS production in these cells. Here we provide evidence that this ROS burst damages mitochondria by causing profound loss of the important mitochondrial inner membrane (IM) lipid, cardiolipin (diphosphatidyl glycerol; Paradies et al., 1997; Polyak et al., 1997). Additionally, we show that while individual mitochondria in NGF-deprived sympathetic neurons underwent little morphological alteration during the period of cardiolipin loss, total mitochondrial mass declined. This decline was, most likely, caused by engulfment of damaged mitochondria by autophagosomes. Consistent with a role for caspases and ROS in this decline, the loss of cardiolipin and mitochondrial mass was inhibited by caspase antagonists and blocked by antioxidant agents. These findings suggest that one means by which caspases disassemble NGF-deprived sympathetic neurons is by irreversibly damaging mitochondria through augmentation of ROS production.

EXPERIMENTAL PROCEDURES

Reagents

Nonyl Acridine Orange (NAO), *cis*-parinaric acid, 1,1′-dioctadecyl-3,3,3′,3′-tetramethylindocarbocyanine perchlorate ($DiIC_{18}$), and Mitotracker Red CMXRos were purchased from Molecular Probes (Eugene, OR, USA). Caspase inhibitor, boc-aspartyl(OMe)-fluoromethylketone (BAF), was purchased from Enzyme Systems Products (Livermore, CA, USA), NGF 2.5S was from Harlan Bioproducts (Indianapolis, IN, USA). The [^{3}H]arachidonic acid was from American Radiolabeled Chemicals, Inc. (St. Louis, MO, USA). All other reagents were purchased from Sigma (St. Louis, MO, USA) unless otherwise stated.

Culture of sympathetic neurons

Timed-pregnant Sprague–Dawley rats were purchased from Harlan Bioproducts (Indianapolis, IN, USA). Superior cervical ganglia were dissected from fetuses on embryonic day 20 or 21. Neurons were dissociated from the ganglia and maintained in cell culture as described (Johnson and Argiro, 1983; Franklin et al., 1995; Franklin and Johnson, 1998). Culture medium contained Eagle's minimum essential medium with Earle's salts (Life Technologies, Inc., Gaithersburg, MD, USA) supplemented with 10% fetal bovine serum, 100 U/ml penicillin, 100 μg/ml streptomycin, 20 μM fluorodeoxyuridine, 20 μM uridine, 1.4 mM L-glutamine, and 50 ng/ml 2.5S NGF. Cells for metabolic labeling assays were plated on a collagen substrate in 24-well Costar tissue culture dishes (Corning, Inc., Corning, NY, USA). Those used for fluorescent or confocal microscopy were plated on a collagen substrate coated on #1 glass coverslips glued with silastic medical adhesive (Dow Corning, Midland, MI, USA) over holes cut in the bottoms of 35 mm Falcon tissue culture dishes (Beckton Dickinson, Franklin Lakes, NJ, USA). One-half to one ganglion was plated per culture in all experiments except for those cultures to be used for immunoblot experiments where 2.5–3 ganglia were plated and those to be used for thin layer and gas chromatography where 25 ganglia were plated. Ganglia for immunoblots and thin layer and gas chromatography were plated on collagen-coated 35 mm and 100 mm Falcon tissue culture dishes respectively. For thin layer and gas chromatography experiments, cells were first plated for 1 h on the collagen substrate in 25–35 μl spots of culture medium. Enough culture medium was then added to cover the plate (15 ml). This procedure resulted in about 40 separate islands of cells per culture dish and was necessary to prevent clustering and detachment of all plated cells from the substrate. NGF was withdrawn from cells by incubating cultures in the standard culture medium lacking NGF and containing a polyclonal NGF-neutralizing antibody (Harlan Bioproducts, Indianapolis, IN, USA; 20). Experiments were begun when cells had been in culture for 6–9 days.

All efforts were made to minimize both the suffering and number of animals used. Experiments conformed to US guidelines on the ethical use of animals.

Confocal and fluorescent microscopy

Confocal imaging was accomplished with a Bio-Rad MRC 1024 laser scanning confocal microscope mounted on a Nikon Diaphot 200 inverted microscope as described (Kirkland and Franklin, 2001). The confocal microscope was controlled by 24-bit MRC-1024 Laser Sharp Software (version 3.0; Bio-Rad, Hercules, CA, USA) running on a Compac Prosignia 300 computer. Visualization of neurons was accomplished with a 60× -plan oil immersion lens (N.A. 1.4).

All fluorescence microscopy was done with a Nikon TE300 inverted microscope as described (Kirkland and Franklin, 2001). The light source was a mercury lamp. Images were captured by a cooled CCD camera (MicroMAX; Princeton Inst., Trenton, NJ, USA) using Metamorph software (Universal Imaging Co., West Chester, PA, USA) running on a Compaq 400 MHz computer. Filter cubes were changed manually except for the 340 ± 15 nm excitation filter that was changed with a Lambda 10-2 optical filter changer (Sutter Instrument Co., Novato, CA, USA). Excitation and emission wavelengths of the FITC filter cube were 480 ± 40 and 535 ± 50 nm respectively. The dichroic mirror was 505 nm. Excitation and emission wavelengths of the TRITC filter cube were 535 ± 50 and 610 ± 75 nm respectively. The dichroic mirror was 565 nm. All microscopy was done at room temperature.

NAO staining

Cellular cardiolipin content was estimated by confocal microscopic visualization of single cells stained with NAO, a dye that binds with high affinity to cardiolipin. This dye is unable to bind to zwitterionic phospholipids and has a very low affinity for other anionic phospholipids. NAO binds to acidic phospholipids through interaction between its quaternary amine and the phospholipid phosphate residue. Cardiolipin contains two phosphate groups per molecule with which NAO forms a dimer. NAO binds onto monoacidic phospholipids with 1:1 stoichiometry. The dimer formation greatly increases cardiolipin affinity for NAO ($K_\alpha = 2\times10^6$ M^{-1} for cardiolipin and $K_\alpha = 7\times10^4$ M^{-1} for monoacidic phospholipids). These characteristics, as well as the high cellular permeability and low toxicity, make NAO an excellent probe for investigating mitochondrial cardiolipin content in living cells (Petit et al., 1992, 1994; Polyak et al., 1997). Cultures were exposed for 10 min to NAO (0.5 or 1 μM) in the appropriate experimental medium and then washed two times with Leibovitz's L-15 medium containing the appropriate treatment. Excitation of NAO was done with the 488-nm line of the confocal microscope. Image acquisition was accomplished with the FITC photomultiplier of the confocal microscope.

Neurons were chosen at random and scanned by the confocal microscope at a resolution of 512×512 pixels. Eight to ten separate fields of view were scanned per culture. Quantification of NAO intensity was accomplished with Sigmagel software (SPSS Science, Chicago, IL, USA) by measuring raw pixel intensity in a 60 μm^2 area of the neuronal soma. Typically, three to five squares with an area of 60 μm^2 tiled almost the entire soma of a cell, excluding the nucleus. In all cases, the square with the highest measured intensity was used for quantification. In most cases, little variation was observed in a single cell in the intensity of the different squares. An alternate criterion for selecting the squares (i.e. choosing the least intense 60 μm^2 square) did not modify the data. The nucleus did not stain with NAO and was therefore excluded from the analysis. The intensity of each neuron was normalized, as described (Kirkland and Franklin,

2001), to that of the average intensity of control neurons maintained in medium containing NGF. Publication images were prepared with Adobe Photoshop 5.0 (Adobe Systems Inc., San Jose, CA, USA).

Arachidonic acid release

Cultures were metabolically labeled with [^{3}H]arachidonic acid by incubation for 24 h in culture medium containing NGF and 1.34 μCi/ml [^{3}H]arachidonic acid. This treatment did not adversely affect the cells. After washing three times with cold medium, cells were either maintained in 500 μl of culture medium containing NGF or deprived of NGF and maintained in 500 μl of medium containing no NGF and anti-NGF antibody. At different times after withdrawal all medium was taken from each well, placed in 1 cc syringes, and forced through 0.2 μM filters (acrodisc). Cultures were then washed three times with cold medium. After washing, 500 μl of cold experimental media was added back to each well. The filtering procedure was done to remove any pieces of degraded cells floating in the medium that might contain [^{3}H]arachidonic acid. Thus, only soluble counts due to released [^{3}H]arachidonic acid or a metabolic product of arachidonic acid were contained in the filtrate. Two hundred microliters of the filtrate was placed in 5 ml of scintillation fluid and [^{3}H] released into the medium was detected by scintillation counting. Released [^{3}H] was normalized to the average amount incorporated into cultures at the beginning of the experiment. This amount was determined by lysing cultures (with 1% Triton in phosphate-buffered saline) at the end of incorporation and measuring radioactivity in the lysate.

Lipid analysis

Ganglia were removed from the substrate with a cell scraper and kept in ice-cold L-15 medium containing appropriate treatments until analysis. Lipids were analyzed by thin layer chromatography and gas chromatography as described (Rao et al., 2000, 2001). In brief, cell suspensions were centrifuged ($1500\times g$ for 5 min), and lipids from pelleted cells were extracted into chloroform/methanol (1:2, v/v) containing 0.01% butylated hydroxytoluene. The entire extract was concentrated under a stream of nitrogen and applied to a silica gel GHL thin layer chromatography plate (Analtech, Newark, DE, USA), which was developed in chloroform/methanol/acetone/ammonium hydroxide (60:28:20:2.5, by volume). Phosphatidylethanolamine, phosphatidylcholine, and cardiolipin were identified using authentic standards, then converted to methyl esters by heating at 70°C for 30 min in 1 ml methanol containing 20 μl concentrated sulfuric acid, 0.01% butylated hydroxytoluene, and 10 nmol of heptadecanoic acid as internal standard. The methyl esters were extracted into hexane and analyzed with a Hewlett Packard 6890 gas chromatograph. Quantification was based on external standard calibration with heptadecanoic acid as an internal standard.

Metabolic labeling with cis-parinaric acid

The small amount of material available in cultures of sympathetic neurons precluded use of standard biochemical assays for lipid peroxidation. For example, the thiobarbituric acid test (Halliwell and Gutteridge, 2000) could not detect peroxidation products even in positive controls where peroxidation was induced by hydrogen peroxide. Therefore, we used the more sensitive single-cell technique of *cis*-parinaric acid fluorescence loss to detect peroxidation. This fluorescent fatty acid is metabolically incorporated into cell membranes. Upon oxidation, the fluorescence is lost (Hockenbery et al., 1993). Neurons were exposed for 24 h to standard culture medium containing NGF and 5 μM *cis*-parinaric acid. They were then washed two times with the same medium lacking the label and incubated in unlabeled culture medium containing NGF for 6 h to allow complete washout of unincorporated *cis*-parinaric acid. Cultures were then exposed to the experimental treatments. At the end of experiments, neurons were placed on the fluorescent microscope and excited at 340 ± 15 nm. The fura-2 filter cube of the microscope was used for emission. Cytoplasmic staining for *cis*-parinaric acid was homogeneous. Consistent with the presence of fewer membranes, the nucleus exhibited much less intense staining than did the cytoplasm. Therefore, the intensity of *cis*-parinaric acid was quantified only in the cytoplasm. Fluorescence intensity was determined in a 33 μm^2 area of the soma of each cell with the Metamorph elliptical region tool. To correct for cellular autofluorescence, the average fluorescence intensity of unlabeled neurons receiving the experimental treatments was subtracted from that of the labeled cells. The intensity of *cis*-parinaric acid measured in cells at the beginning of experiments was used for normalization.

Electron microscopy (EM)

Neurons for EM were plated on collagen-coated #1 coverslips. After experiments, cultures were fixed for 1–2 h at room temperature or overnight at 4°C in 0.1 M phosphate buffer (pH 7.2) containing 2% glutaraldehyde and 2% formaldehyde. Cultures were post-fixed for 1 h at room temperature with 0.1 M phosphate buffer containing 2% osmium tetroxide. After dehydration in a graded series of alcohol solutions and embedding in Durcupan (Fluka, Switzerland), the coverslips were removed by etching with hydrofluoric acid. Sections (70 nm) were cut parallel to the coverslips then post-stained with uranyl acetate and lead citrate before examination with a Philips CM120 transmission electron microscope.

Areas within scanned images of electron micrographs were measured using the Metamorph tracing tool. Each mitochondrion was carefully outlined and the area within the traced region determined. The cytoplasmic area of each micrograph was also ascertained by tracing the entire cytoplasmic region, excluding the nucleus. All areas were calibrated to scale bars on the micrographs.

Hsp60 immunoblots

At the end of experiments, cultures were washed one time with Tris-buffered saline (TBS; pH 7.6). The cells were then removed from the substrate with a cell scraper and transferred in 1.0 ml TBS to a 1.5 ml microfuge tube. The samples were next pelleted at $5000\times g$ for 1 min at room temperature. The supernatants were removed and 100 μl of lysis buffer consisting of 25% glycerol, 60 mM Tris (pH 6.8), 100 mM dithiothreitol, 1 mM EDTA, 0.1% Bromophenol Blue, 0.2% sodium dodecyl sulfate, and a 1:100 dilution of a protease inhibitor cocktail (Calbiochem #539134, La Jolla, CA, USA) added. The pellets were then homogenized for 15 s with a disposable pellet pestle (Kontes, Vineland, NJ, USA). After homogenization, samples were boiled for 5 min, allowed to return to room temperature, and then spun for 1 min in an Eppendorf 5414 table-top centrifuge to pellet debris. Thirty microliters of the lysates were loaded into the wells of 10% Tris–HCl pre-cast gels (Bio-Rad). Prestained molecular weight markers (7 μl; Bio-Rad) were loaded into one lane. Gels were run for ∼40 min at 180–200 V. Proteins were transferred from the gels onto polyvinylidene difluoride membranes (Millipore, Bedford, MA, USA) overnight at 4°C. The membrane was briefly equilibrated in TBS, placed in blocking buffer consisting of 0.2% I-Block (CDP-Star, Tropix, Bedford, MA, USA) and 0.1% Tween-20 in TBS and was gently shaken at 4°C for 0.5 h. The membrane was then incubated in 200–500 ng/ml mouse anti-Hsp60 monoclonal antibody (StressGen Biotechnologies, Victoria, BC, Canada) for 1 h at room temperature. Next, the membrane was washed in blocking buffer (two times 2 min+four times 5 min) followed by incubation for 60 min at room temperature in the secondary antibody (1:5000) provided with the kit. The membrane was then washed in blocking buffer as before and washed twice with the CDP-Star kit assay buffer. The CDP-Star kit substrate was layered onto the membrane for 5 min, then drained off. The membrane was placed in Saran Wrap and

the molecular weight markers indicated on the plastic with a phosphorescent pen. The blot was then exposed to X-ray film. Quantification of scanned blots was done with SigmaGel (SPSS Science, Chicago, IL, USA).

Statistical analysis

Appropriate statistical measures were determined for each data set based on experimental technique and sample distribution. For most statistical comparisons, Kruskal–Wallis one-way analysis of variance (ANOVA) on ranks was the appropriate statistical measure. Where necessary, Dunn's multiple comparisons test was also performed. This type of analysis was used in all cases unless otherwise stated. All statistics were performed with SigmaStat (SPSS Science). The null hypothesis was rejected at the 0.05 level. All figures show means ± S.E.M.

RESULTS

Loss of cardiolipin from mitochondria after NGF withdrawal

The fluorescent dye, NAO, binds with high affinity to the mitochondrial IM lipid, cardiolipin. Because NAO does not bind significantly to any other cellular component, it serves as an excellent marker for estimating cellular cardiolipin content (Petit et al., 1992, 1994; Paradies et al., 1997; Polyak et al., 1997). The binding of NAO to mitochondria in rat sympathetic neurons has not yet been investigated. To determine whether NAO stains mitochondria of these cells, we double-labeled cultures with NAO and the mitochondria-specific marker, Mitotracker Red CMXRos (Neame et al., 1998). Both of these dyes exhibited a punctate staining pattern in the neuronal soma with no staining in the nucleus, consistent with mitochondrial localization. There was little overlap of the emission spectra of the two dyes (not shown). Thus, Mitotracker Red CMXRos could be used to label mitochondria and determine if NAO staining was restricted to mitochondria. Figure 1A shows that the patterns of staining of the two dyes in a single neuronal soma were nearly identical. Consistent with the low affinity of phospholipids other than cardiolipin for NAO, there was little non-mitochondrial NAO staining. It has been reported that changes in mitochondrial membrane potential can affect NAO staining in some cell types (Keij et al., 2000). To determine if altering mitochondrial membrane potential affected NAO staining in sympathetic neurons we depolarized mitochondria by treating cultures with the protonophore, carbonyl cyanide *p*-trifluoromethoxyphenylhydrazone (FCCP). Cells were exposed for 30 min to medium containing FCCP (5 μM) and Mitotracker Red CMXRos (20 ng/ml). Ninety-two percent of control cells displayed punctate staining similar to that shown in Fig. 1A while only 9% of FCCP-treated cells did ($n = 148$ and 162 cells respectively). Because Mitotracker Red CMXRos stains only mitochondria that have a membrane potential (Neame et al., 1998), the decrease in number of stained cells in FCCP-treated cultures indicated profound loss of mitochondrial membrane potential. Similar treatment with FCCP did not significantly decrease average NAO

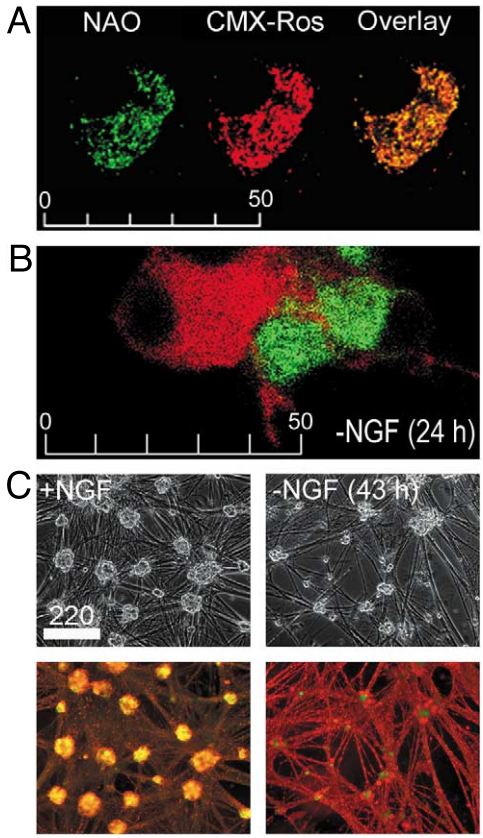

Fig. 1. Loss of the mitochondrial IM lipid, cardiolipin, from NGF-deprived rat sympathetic neurons in cell culture. (A) NAO, a highly specific stain for cardiolipin, labeled mitochondria in sympathetic neurons. Confocal micrographs showing co-localization of NAO with the mitochondrial stain, Mitotracker Red CMXRos, in a single neuronal soma. Left and middle micrographs show NAO and Mitotracker CMXRos staining respectively. The final micrograph is an overlay of the first two. Yellow indicates extensive areas of overlap (e.g. mitochondria). Cultures were exposed to 20 ng/ml Mitotracker CMXRos for 20 min. Image acquisition was accomplished with the TRITC photomultiplier of the confocal scope. NAO staining is described in Experimental procedures. All scale bars in this figure are in μm. (B) Confocal micrographs of neurons deprived of NGF for 24 h and double-stained with NAO and $DiIC_{18}$. Loss of NAO staining after NGF deprivation suggested loss of cardiolipin. The non-specific membrane dye $DiIC_{18}$ was used as a counterstain to enhance visualization of cells that had lost NAO staining. The FITC and TRITC channels of the confocal scope were used to separate NAO and $DiIC_{18}$ emissions. Cultures were exposed to 10 μg/ml $DiIC_{18}$ for 25 min. During the last 10 min of exposure, cells were stained with NAO as described in Experimental procedures. Red indicates areas of no NAO staining (large cell at left). Green shows areas of NAO staining overlying $DiIC_{18}$ staining (two cells on the right). (C) Micrographs demonstrating that most cell bodies and all neurites lost NAO staining during apoptotic death caused by NGF withdrawal. Top and bottom photos are matched phase-contrast and fluorescent micrographs of the same fields of view. Cultures were double-labeled with NAO and $DiIC_{18}$ as in (B). Yellow or green in the NGF-maintained cells indicates areas of overlap between the staining patterns of the two dyes. In the cells deprived of NGF for 43 h, $DiIC_{18}$ staining remained intense (red). Little NAO staining (yellow or green) was apparent. The neurons that stained green at 43 h after deprivation may have consisted of the subpopulation of these cells that are resistant to apoptotic death after NGF withdrawal (Deckwerth and Johnson, 1993). FITC (NAO) and TRITC ($DiIC_{18}$) filter cubes were used to separate the excitation and emission spectra of the two dyes. Micrographs are overlays of the two. Scale bar applies to all micrographs.

staining intensity (16 ± 3% decline, $n = 114$ neurons, $P > 0.07$ compared to control). The NAO intensities were normally distributed in the population of cells (Kolmogorov–Smirnov test) with < 1% of cells showing NAO staining intensity < 25% of the control average, a value similar to that observed in the population of control cells. The co-localization of NAO and Mitotracker Red CMXRos staining and the insignificant effect of changing mitochondrial membrane potential on staining suggests that, as in many other cell types, NAO specifically stains the mitochondria of rat sympathetic neurons by binding onto mitochondrial cardiolipin.

Phase-contrast and fluorescence microscopy of neurons deprived of NGF for 6–12 h showed no obvious changes in morphology or NAO staining. However, as previously reported (Deckwerth and Johnson, 1993; Franklin and Johnson, 1998), by 18 h after withdrawal, most neurons had undergone profound atrophy (not shown). By 24 h after deprivation, NAO stained many cells lightly, or not at all, suggesting that a subpopulation of neurons had lost cardiolipin by this time (Fig. 1B). Most sympathetic neurons in cultures deprived of NGF for > 36 h are dead and remain in the culture dish as enucleate ghosts or as debris (Martin et al., 1988; Deckwerth and Johnson, 1993; Edwards and Tolkovsky, 1994). Only a few of the somas of cells in these cultures and none of the neurites could be stained with NAO, suggesting that most or all neurons eventually lost all cardiolipin during the apoptotic process (Fig. 1C).

Figure 2A shows a quantification of the time-course of changes in NAO staining after NGF deprivation. No clear alterations of staining were apparent during the first 6 h subsequent to NGF removal. However, by 12–18 h after withdrawal, the pattern of NAO staining had changed dramatically. By this time, many cells had NAO staining intensities that were either higher or lower than those of cells maintained in medium containing NGF. By 24 h after NGF deprivation, there was a bimodal distribution of NAO staining intensities ($P < 0.003$

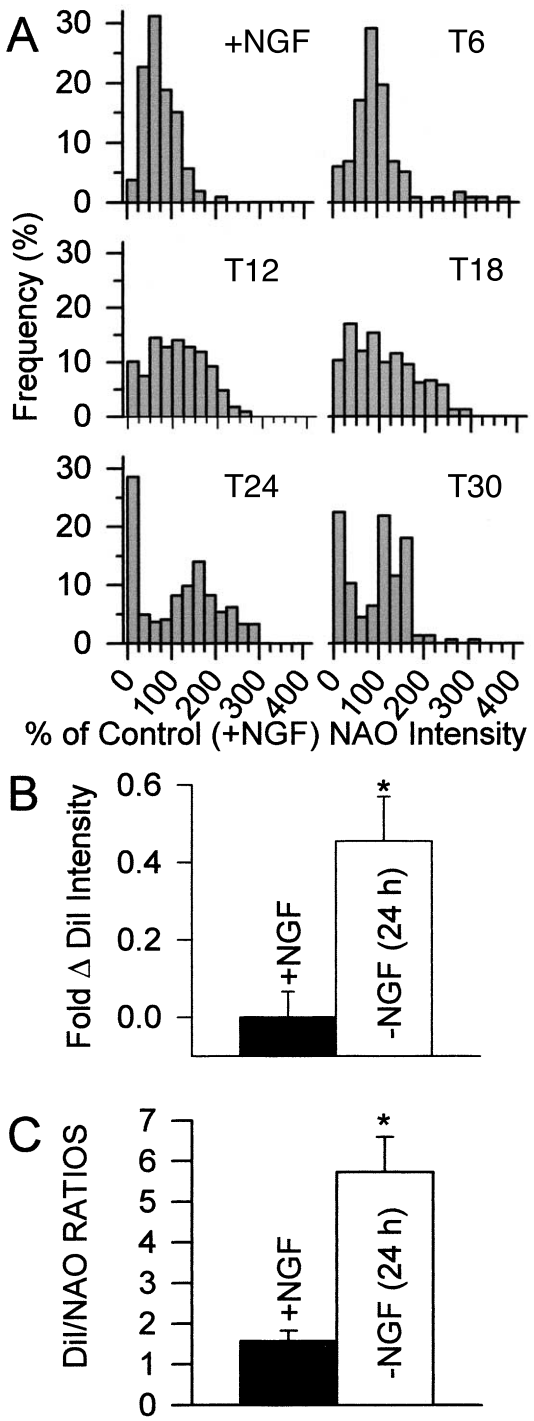

Fig. 2. Alterations in NAO staining intensity after NGF withdrawal. (A) Clear differences in intensity were observed by 12–18 h after NGF deprivation. Data are shown as frequency histograms made up of bins that are in 25% increments of the average NAO intensity in NGF-maintained cells. For example, the bar on the left of each graph represents the percentage of NGF-deprived neurons that had 0–25% of the average NAO intensity of NGF-maintained cells at that time-point. The next bar to the right represents the percentage of NGF-deprived neurons with 25–50% of control NAO intensity and so on. Raw NAO intensity values (in arbitrary units) for control cells in a representative experiment ranged between 40 044 and 59 894 while cells from the same plating deprived of NGF for 24 h had a range of 2825–68 667. $n = 95$–258 neurons from three separate platings for the different time-points. (B) Average $DiIC_{18}$ staining intensity increased slightly by 24 h after NGF withdrawal. This increase probably occurred because cytoplasmic membranes stained by $DiIC_{18}$ were concentrated into a smaller volume as a result of somatic atrophy. $DiIC_{18}$ staining was done as described in Fig. 1B. (C) The $DiIC_{18}$:NAO ratio greatly increased over the same period suggesting major loss of cardiolipin relative to other lipid components of cellular membranes. Ratios were determined on a cell-by-cell basis. The NAO and $DiIC_{18}$ intensities were measured in the same area of the cytoplasm of each cell. These ratios provide a rough estimate of loss of NAO/cardiolipin from membranes relative to other loss of other membrane lipids. It was not possible to ratio NAO to other mitochondrial dyes or markers. Mitotracker Red CMXRos and most other mitochondrial dyes are dependent on mitochondrial membrane potential which is lost during the apoptotic death of these cells. Immunocytochemical markers for mitochondria also could not be used as the detergent treatment necessary for antibody permeabilization abolished NAO staining. $n = 125$ from three separate platings for each condition in (A) and (B). Asterisks indicate statistical difference ($P < 0.001$) from cells maintained in the presence of NGF.

for average raw intensities at 24 h after deprivation compared to t0 (+NGF) control). One group of these neurons (~28%) did not stain for NAO at all, suggesting that they had lost almost all cardiolipin. Another population of neurons exhibited control or increased NAO staining intensities. The striking atrophy that occurs in these cells by 24 h after NGF deprivation (Franklin and Johnson, 1998) may have concentrated NAO-stained mitochondria into a smaller volume and caused the increase of NAO staining intensities in some cells.

Because some NGF-deprived neurons exhibited increased NAO staining while others showed greatly decreased staining, average NAO intensity of the entire population of cells was not very informative. In an endeavor to obtain a meaningful average of changes in NAO staining intensity in the population of cells and to estimate NAO/cardiolipin loss relative to other membrane lipids, we stained neurons with both NAO and the lipophilic dye, $DiIC_{18}$. The $DiIC_{18}$ treatment resulted in intense staining of membranes throughout the cells. The staining intensity of $DiIC_{18}$ changed little after NGF deprivation, even in cells where NAO staining was completely lost (Fig. 1B) suggesting that cardiolipin was selectively lost while most other lipids were not. Figure 2B shows that the average staining intensity of $DiIC_{18}$ increased on average about 0.4-fold ($P < 0.001$) in cells deprived of NGF for 24 h. This increase was, again, probably caused by concentration of membranes secondary to atrophy. To measure NAO loss relative to loss of other membrane lipids labeled by $DiIC_{18}$, we quantified both NAO and $DiIC_{18}$ staining intensities in the same area of the cytoplasm of single, double-labeled cells. Figure 2C shows that average single-cell $DiIC_{18}$:NAO ratios increased by about six-fold ($P < 0.001$) within 24 h of NGF withdrawal. This finding further illustrates that there was extensive loss of NAO staining in cells deprived of NGF and suggests selective loss of cardiolipin compared to other cellular lipids.

To obtain a more direct and quantitative estimate of cardiolipin content relative to other membrane phospholipids, we used gas chromatography to measure cardiolipin, phosphatidylcholine, and phosphatidylethanolamine concentrations in control and NGF-deprived cultures (Table 1). The combined concentration of the three lipids decreased about 46% by 24 h after NGF withdrawal ($P < 0.05$ by Mann–Whitney rank sum test). Cardiolipin concentration decreased to a greater extent than did the concentrations of either phosphatidylcholine or phosphatidylethanolamine (Table 1). Thus, while a global loss of lipids occurred after NGF deprivation, the decrease of cellular cardiolipin content was greater than that of these two other major membrane phospholipids suggesting that cardiolipin was selectively lost from cells. The combined data suggest that loss of NAO staining after NGF deprivation was caused by an actual loss of cardiolipin from mitochondria.

The global loss of phospholipids in NGF-deprived cultures could have been caused by increased lipid degradation, by loss of membranes into the culture medium due to cellular disruption, by decreased lipid synthesis without a concurrent reduction in normal lipid turnover, or by a combination of any or all of these possibilities. To determine whether loss of lipids after NGF withdrawal could be accounted for by increased lipid degradation, we metabolically labeled cells with [^{3}H]arachidonic acid and then deprived them of NGF. Arachidonic acid is incorporated into membrane phospholipids where it is stored as a glycerol ester. Hydrolysis of phospholipids by pathways involving phospholipases A_2, C, and D liberates arachidonic acid. Because phospholipids are major components of all cell membranes, measurement of arachidonic acid release from metabolically-labeled cells is a sensitive measure of overall lipid loss from cellular membranes. Figure 3 shows that rate of release of soluble [^{3}H] from arachidonic acid-labeled cells did not change significantly after NGF deprivation, suggesting no increase in overall phospholipase activity or membrane degradation after NGF withdrawal. Therefore, global lipid loss reflected either cellular disruption or normal lipid degradation without lipid replacement. To determine if loss of membranes into the culture medium secondary to cellular disruption occurred, we lysed cells at the end of experiments and measured remaining amount of incorporated [^{3}H]. The amount of radiolabel remaining in NGF-deprived cultures combined with soluble counts measured in the medium accounted for 104 ± 7% of the initial amount of [^{3}H]arachidonic acid initially incorporated into the cells. These data indicate that there was no cellular disruption and subsequent loss of membranes. Therefore, global loss of lipids appears to have occurred

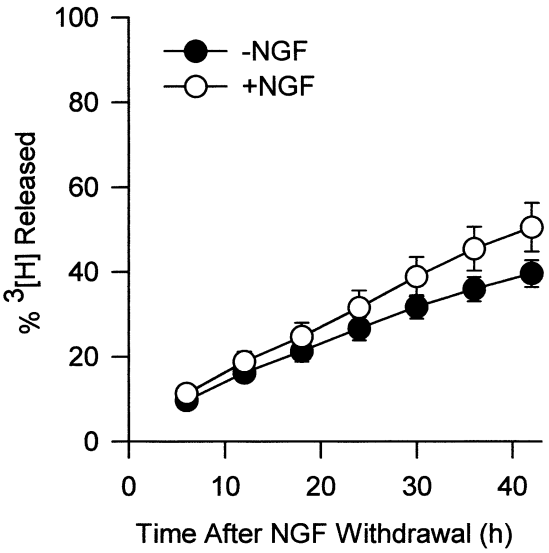

Fig. 3. Rate of [^{3}H] released from [^{3}H]arachidonic acid-labeled cultures did not increase after NGF deprivation indicating no elevation of phospholipase activity. Data are shown as cumulative release of the total amount of [^{3}H] incorporated into cells at the end of metabolic labeling. Total incorporation was determined from lysates of cultures taken at the end of labeling. Cumulative release was determined for each culture separately. Rate of release of [^{3}H] from cultures deprived of NGF was not significantly different from the rate of release from cultures maintained in medium containing NGF ($P > 0.05$ by Kruskal–Wallis one-way ANOVA on Ranks with Dunn's all pairwise multiple comparisons procedure). $n = 10$ cultures from two separate platings for each time-point.

by decreased lipid synthesis without a concurrent reduction in normal lipid turnover. Because cardiolipin is a small component of total cellular phospholipids, it did not contribute substantially to the released [^{3}H]arachidonic acid shown in Fig. 3. The greater decrease of cardiolipin concentration than of phosphatidylethanolamine and phosphatidylcholine concentrations after NGF withdrawal as revealed by the gas chromatographic experiments could be explained by a faster rate of turnover of this lipid compared to that of the two other lipids. However, the profound loss of NAO staining in many cells suggests a selective loss that is more easily explained by an increased rate of cardiolipin degradation.

Lipid peroxidation increased after NGF deprivation

Withdrawal of NGF from rat sympathetic neurons in cell culture induces their mitochondria to increase production of ROS (Greenlund et al., 1995; Dugan et al., 1997; Kirkland and Franklin, 2001). Because cardiolipin is unsaturated, it is particularly susceptible to lipid peroxidation via ROS attack (Hockenbery et al., 1993; Polyak et al., 1997). Moreover, cardiolipin is found only in the mitochondrial IM, the location of most cellular ROS production, making it even more susceptible to ROS damage. Indeed, loss of NAO staining during apoptosis is sometimes taken as an indication of ROS-induced cardiolipin peroxidation and destruction of the mitochondrial IM (Polyak et al., 1997; Poot and Pierce, 1999). A sustained increase of mitochondrial-derived ROS in rat sympathetic neurons in culture begins about 12 h after NGF deprivation and increases in magnitude throughout the remainder of the apoptotic process (Kirkland and Franklin, 2001). This ROS burst is concurrent with loss of NAO staining suggesting the possibility of a causal relationship. To determine if lipid peroxidation occurred in NGF-deprived cells, we metabolically labeled cellular membranes before deprivation with the peroxidation-sensitive unsaturated fatty acid, *cis*-parinaric acid (Hockenbery et al., 1993). Upon peroxidation, *cis*-parinaric acid fluorescence is lost. Figure 4A, B shows that the fluorescence intensity in the somas of *cis*-parinaric acid-loaded cells decreased during the same period that ROS levels increase. By 12–24 h after NGF withdrawal, elevated cellular fluorescence caused by incorporated *cis*-parinaric acid had declined by as much as 50% suggesting the occurrence of significant lipid peroxidation. *Cis*-parinaric acid fluorescence did not decrease in the somas of cells maintained in medium containing NGF.

All atrophy in NGF-deprived sympathetic neurons in culture occurs between 12 and 24 h after NGF withdrawal (Franklin and Johnson, 1998) while most of the decline in *cis*-parinaric intensity occurred by 12 h after NGF deprivation. Presumably, few membranes are lost from the somas of these cells before atrophy has occurred. Little additional decline in *cis*-parinaric intensity occurred during the period of atrophy. Therefore, it is unlikely that the decrease of *cis*-parinaric fluorescence in NGF-deprived cells was caused by global loss of membranes (Table 1). Consistent with loss of *cis*-parinaric intensity not being caused by global membrane loss, $DiIC_{18}$ staining had increased slightly by 24 h after NGF withdrawal (Fig. 2B), probably because of concentration of the membranes remaining in the shrunken somas into a smaller volume. The ratio of saturated to unsaturated fatty acids in the cells increased after NGF withdrawal indicating selective loss of unsaturated fatty acids (Table 1). This finding is consistent with peroxidation occurring after NGF withdrawal because unsaturated fatty acids are more susceptible to ROS attack than are saturated fatty acids (Halliwell and Gutteridge, 2000). Treatment of NGF-maintained cultures with H_2O_2 (10 mM for 1 h; Kirkland and Franklin, 2001) to induce lipid peroxidation decreased *cis*-parinaric acid intensity to $68 \pm 7\%$ of control intensity ($P < 0.001$). Therefore, the most likely mechanism for the loss of *cis*-parinaric acid fluorescence in NGF-deprived neurons was lipid peroxidation induced by increased levels of ROS (Kirkland and Franklin, 2001).

Caspase inhibitors decrease ROS levels during the apoptotic death of several neuronal cell types (Tan et al., 1998; Kirkland and Franklin, 2001). The broad-spectrum caspase inhibitor BAF (Deshmukh et al., 1996) prevents apoptosis of sympathetic neurons after NGF deprivation and greatly attenuates, but does not prevent, the ROS burst that is concurrent with decreased NAO staining and reduced *cis*-parinaric acid fluorescence (Kirkland and Franklin, 2001). The somas of NGF-deprived cells that were pre-labeled with *cis*-parinaric acid and maintained in a viable state for 24 h with BAF (30 μM) did not show any loss of fluorescence intensity (Fig. 4C). This finding suggests that attenuating

Table 1. Phospholipid analysis

	Concentrations			% Decrease			Sat/Unsa fatty acids
	[C]	[PE]	[PC]	[C]	[PE]	[PC]	
+NGF	3.7 ± 1.1	23.5 ± 4.1	81.3 ± 10.6	–	–	–	1.15 ± 0.03
−NGF	1.7 ± 0.4	13.8 ± 1.9	49.9 ± 2.7	52 ± 4	37 ± 9	37 ± 6	1.25 ± 0.01
−NGF+BAF	2.7 ± 0.5	24.1 ± 6.8	69.0 ± 9.5	35 ± 7	13 ± 10	17 ± 8	1.22 ± 0.06

Cardiolipin (C), phosphatidylethanolamine (PE), phosphatidylcholine (PC), saturated (Sat) fatty acids, unsaturated (Unsa) fatty acids. Numbers in first three columns are average concentrations of C, PE, and PC in nmol/culture ($n = 3$ cultures from three separate platings). The next three columns show average percentage decrease in concentrations of the three phospholipids compared to concentrations in control cultures that were plated at the same time. The last column shows the ratio of the total amount of saturated to unsaturated fatty acids measured in the three phospholipids. This analysis includes phospholipids from both somas and neurites. Cultures were deprived of NGF for 24 h before measurement of lipids.

the ROS burst with the caspase inhibitor also prevented any substantial lipid peroxidation from occurring. Similarly, the protein synthesis inhibitor, cycloheximide (CHX; 1 μg/ml), and the antioxidant compound, *N*-acetyl-L-cysteine (L-NAC); Kirkland and Franklin, 2001; Poot and Pierce, 1999) completely prevented loss of *cis*-parinaric acid fluorescence in neurons deprived of NGF for 24 h (Fig. 4C). Both of these compounds potently

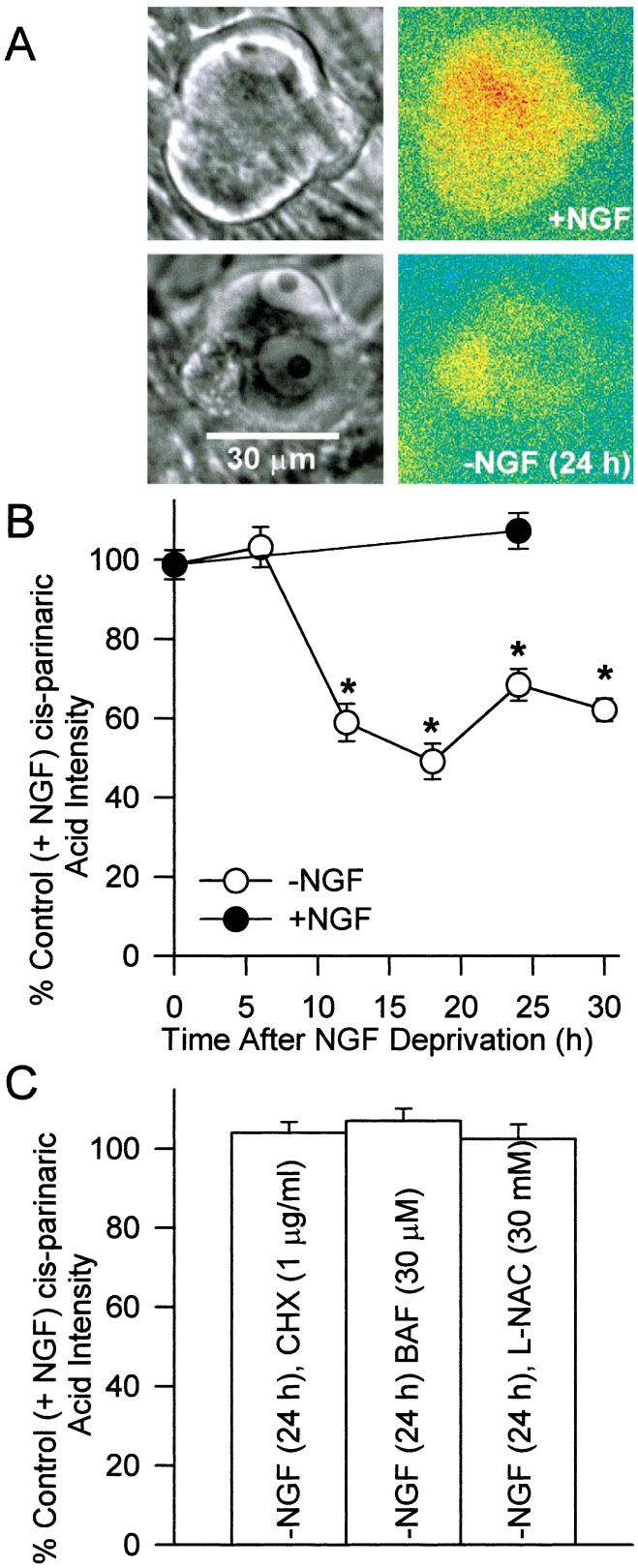

Fig. 4.

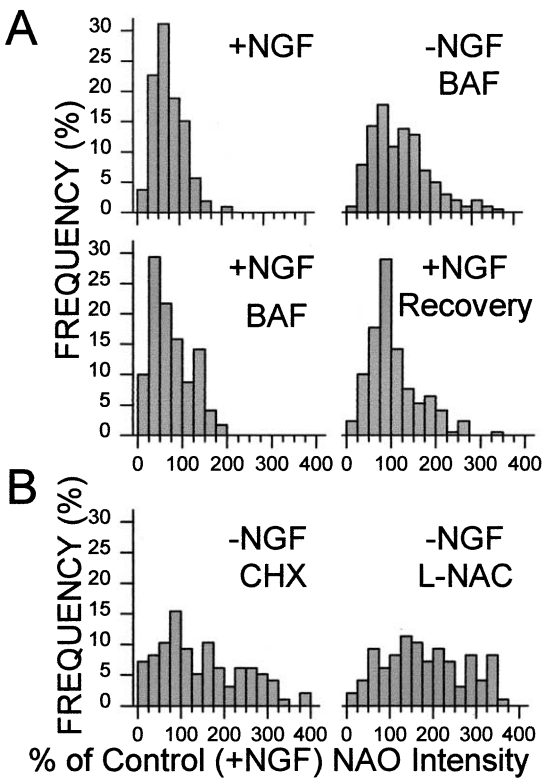

Fig. 5. Loss of NAO staining was blocked by BAF, CHX, and L-NAC. (A) Quantification of changes in the NAO staining pattern of NGF-deprived, BAF-saved neurons. Upper right graph shows NAO staining pattern in neurons deprived of NGF and maintained in BAF (30 μM) for 48 h. The average raw NAO staining intensity of these cells was significantly different from that of control cells maintained in the presence of NGF ($P < 0.001$). NAO staining in neurons maintained for 48 h in culture medium containing BAF and NGF (bottom left graph) was similar to that of control cells without BAF as was that of NGF-deprived neurons that had been maintained in BAF for 3 days and then re-exposed to NGF for 5–7 days (bottom right graph; $P > 0.1$). Few cells die over this period after NGF deprivation in cultures exposed to this concentration of BAF (Deshmukh et al., 1996). $n = 106$–203 neurons from three separate platings for the different time-points. (B) Quantification of changes in the NAO staining intensities of CHX- or L-NAC-saved cells. Cultures were deprived of NGF for 24 h and maintained in optimal survival-promoting concentrations of CHX (1 μg/ml) or L-NAC (30 mM) for this period (Kirkland and Franklin, 2001). The raw NAO staining intensities of these cells were significantly different from the raw intensities of control cells maintained in medium containing NGF ($P < 0.001$). $n = 131$–142 neurons from three platings.

suppress ROS accumulation after NGF deprivation by increasing cellular glutathione concentration (Ratan et al., 1994; Kirkland and Franklin, 2001). They also block caspase activation and apoptosis by inhibiting redistribution of cytochrome *c* from the mitochondrial intermembrane space into the cytoplasm.

BAF, CHX, and L-NAC blocked loss of *cis*-parinaric acid fluorescence after NGF deprivation. If the apparent loss of cardiolipin after withdrawal was caused by similar peroxidation, it should also have been inhibited by these compounds. Figure 6 shows that was the case. Maintenance of NGF-deprived cultures for 2 days in BAF-containing medium prevented any obvious decrease of NAO staining (Fig. 5A). Indeed, many neurons exhibited increased NAO intensity. Because all of these cells were profoundly atrophied (Deshmukh et al., 1996), the enhanced staining was probably caused by concentration of NAO-stained mitochondria into a smaller volume in some cells secondary to atrophy. Re-addition of NGF to the culture medium caused hypertrophy and recovery of control staining pattern over a period of several days, lending credence to this explanation. Another broad-spectrum caspase inhibitor, VAD-CHO (100 μM), also prevented loss of NAO fluorescence (data not shown). Exposure of cultures to CHX and L-NAC from the time of NGF deprivation resulted in an NAO staining pattern similar to that observed in the BAF-supported cells (Fig. 5B). Direct treatment of cultures maintained in the presence of NGF with H_2O_2 (10 mM for 1 h; Kirkland and Franklin, 2001) to induce lipid peroxidation caused NAO fluorescence to decrease to $40 \pm 6\%$ of control intensity ($P < 0.001$ by Mann–Whitney rank sum test). The gas chromatographic data in Table 1 show that BAF treatment inhibited loss of cardiolipin, phosphatidylethanolamine, and phosphatidylcholine from cultures for at least the first 30 h after NGF deprivation. These findings suggest that increased lipid peroxidation was, at least partially, responsible for the general loss of phospholipids after NGF deprivation and of cardiolipin from the mitochondrial IM. Moreover, they suggest that caspase-augmented ROS production was partially responsible for the loss.

Mitochondrial morphology during the period of cardiolipin loss

Because NAO staining is a sensitive indicator of car-

Fig. 4. Increased lipid peroxidation in NGF-deprived neurons. (A) Representative paired (left and right) phase-contrast and pseudo-color micrographs of neurons metabolically labeled with the fluorescent, oxidation-sensitive fatty acid, *cis*-parinaric acid. The intensity of *cis*-parinaric acid fluorescence in cells deprived of NGF for 12–24 h was visibly less than that of cells maintained in NGF for the same period. Red represents the most intense *cis*-parinaric staining, blue the least. (B) Time-course of decrease in *cis*-parinaric acid intensity in NGF-deprived neurons. Cells maintained in medium containing NGF did not show a similar decline in fluorescence intensity. Asterisks indicate significantly different from control intensity measured before NGF withdrawal at t0 ($P < 0.001$). $n = 73$–95 neurons from three separate platings for each time-point. (C) Loss of *cis*-parinaric acid intensity in NGF-deprived cells was blocked by the pan-caspase inhibitor, BAF (30 μM), by the protein synthesis inhibitor, CHX (1 μg/ml), and by the antioxidant, L-NAC (30 mM). These compounds do not prevent the atrophy that occurs after NGF deprivation (Deshmukh et al., 1996; Franklin and Johnson, 1998). Neurons were deprived of NGF for 24 h in the presence of the compounds. For the three treatments, $P > 0.78$ compared to the *cis*-parinaric intensity of cells maintained in medium containing NGF for the same period and $P < 0.001$ compared to intensity of cells deprived of NGF for 24 h. $n = 80$–108 neurons from three platings.

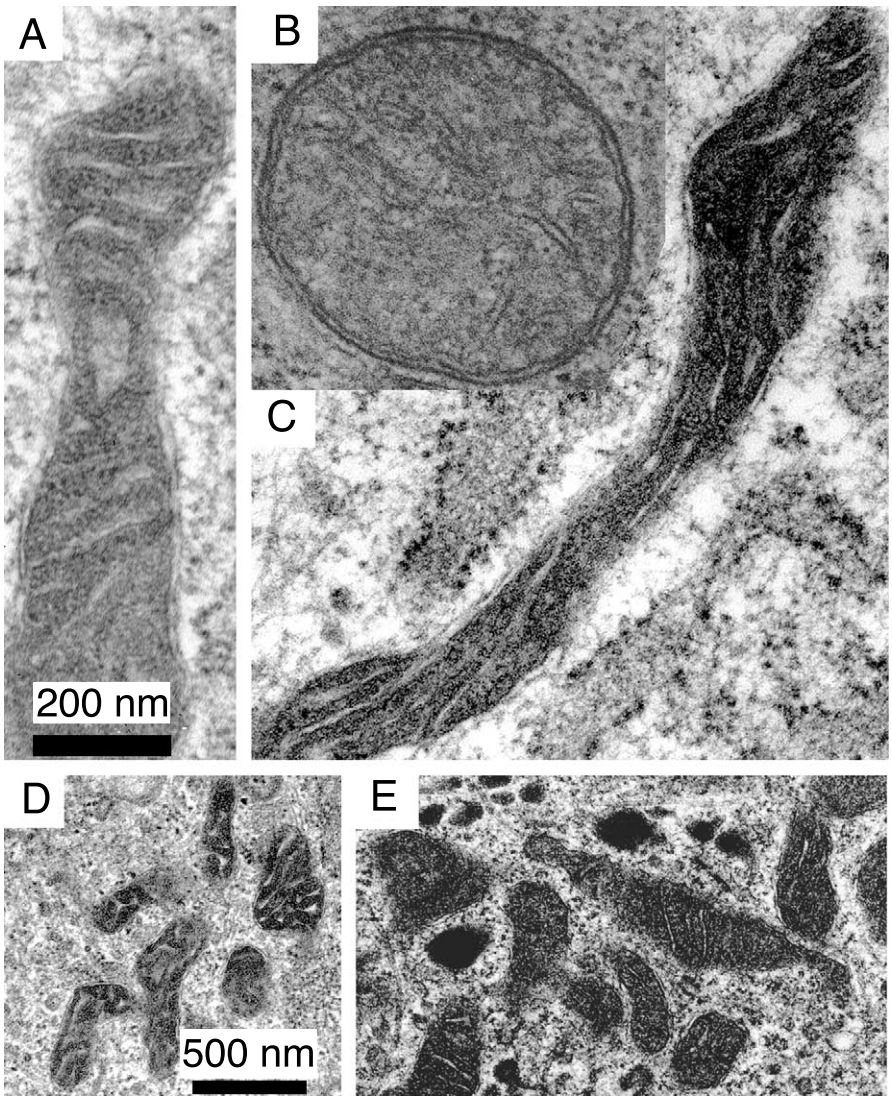

Fig. 6. Electron micrographs of mitochondria in NGF-maintained and -deprived neurons. (A) Mitochondrion in a cell that had been maintained in medium containing NGF. (B) Mitochondrion in a neuron that had been deprived of NGF for 24 h. (C) Mitochondrion in a cell that had been deprived of NGF for 30 h. (D) Micrograph of mitochondria in an NGF-maintained cell. (E) Micrograph of mitochondria in a neuron deprived of NGF for 24 h. The small, dark organelles are lysosomes (Xue et al., 1999). The scale bars for the high magnification micrographs in (A) also apply to the high magnification micrographs in (B) and (C). The scale for (D) and (E) is the same.

diolipin content, and cardiolipin is found in eukaryotic cells only in mitochondria, NAO is sometimes used as a marker for mitochondrial mass (Polyak et al., 1997). Therefore, the striking decrease of NAO staining observed in many neurons deprived of NGF for 24–30 h suggested possible loss of mitochondria in those cells. However, previous work has reported few obvious changes in the mitochondria of week-old rat sympathetic neurons in cell culture after NGF withdrawal (Martin et al., 1988; Martinou et al., 1999). To endeavor to resolve this issue, we performed morphometric electron microscopic analysis of mitochondria in NGF-maintained and -deprived cells. Figure 6 shows electron micrographs of mitochondria in control neurons and in cells deprived of NGF for 24 and 30 h. There were no obvious alterations in mitochondrial morphology by 24 h after NGF withdrawal (Fig. 6A, B). However, by 30 h after withdrawal, many mitochondria exhibited a darkened matrix suggestive of matrix condensation (Fig. 6C). Additionally, the intracristal space in these mitochondria appeared flattened and reduced in volume compared to that in control cells. In no case was swelling of mitochondria apparent. Mitochondria were elongated structures that tended to weave in and out of EM sections. Where a mitochondrion left a section, the OM was not apparent. Because of this sectioning artifact, it was not possible to unambiguously determine if the OM was complete, even in control cells (Fig. 6A, B).

There was a small, but significant, decrease in the average cross-sectional area of individual mitochondria in cells deprived of NGF for 30 h (Fig. 7A; $P < 0.01$). This finding is similar to that of Martinou et al. (1999) who reported a similar decrease of mitochondrial size during the apoptotic death of sympathetic neurons.

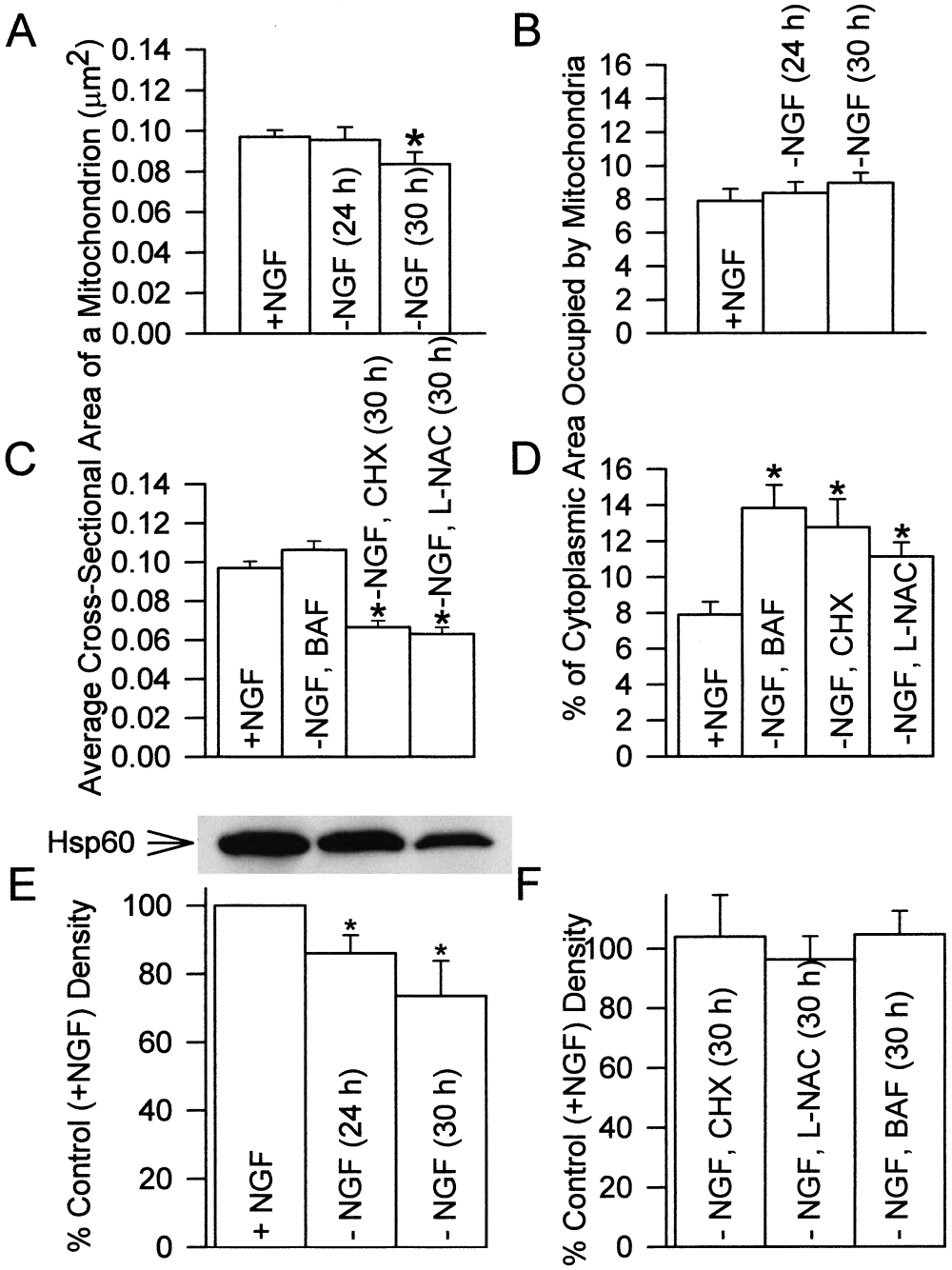

Fig. 7. Quantification of changes in the morphology of mitochondria in neurons deprived of NGF. (A) There was a small, but significant ($P < 0.04$), reduction of the average cross-sectional area of mitochondrial profiles by 30 h after NGF withdrawal. $n = 246$–398 profiles from three platings. (B) The total area of cytoplasm occupied by mitochondrial profiles in electron micrographs did not change significantly ($P > 0.05$) after NGF withdrawal. $n = 31$–39 cellular profiles from three platings. (C) Average cross-sectional areas of mitochondrial profiles in NGF-deprived neurons treated with BAF (30 μM), CHX (1 μg/ml), or L-NAC (30 mM). $n = 333$–461 profiles from three platings. (D) Effects of the treatments in (C) on the percentage of cytoplasm occupied by mitochondrial profiles. $n = 22$–39 cells from three platings. Data in (A–D) were taken from transmission electron micrographs. (E) Changes in the mitochondrial matrix protein, HSP60, after NGF deprivation. Graph is from quantification of western blots of four to seven cultures taken from three to four platings. The lanes in the representative blot are above bars corresponding to the treatments the cultures received. (F) Hsp60 loss was prevented by BAF (30 μM), CHX (1 μg/ml), and L-NAC (30 mM) in cultures deprived of NGF. Graph is combined data of western blots from three cultures taken from three platings.

The percentage of total cytoplasmic area occupied by mitochondrial profiles in electron micrographs did not change significantly during the first 30 h after NGF deprivation (Fig. 7B; $P > 0.05$). At first glance, these data seem to indicate that the total mitochondrial volume per cell was not changed. However, extensive cellular atrophy also occurs by 24–30 h after NGF deprivation (Franklin and Johnson, 1998). Because the measured

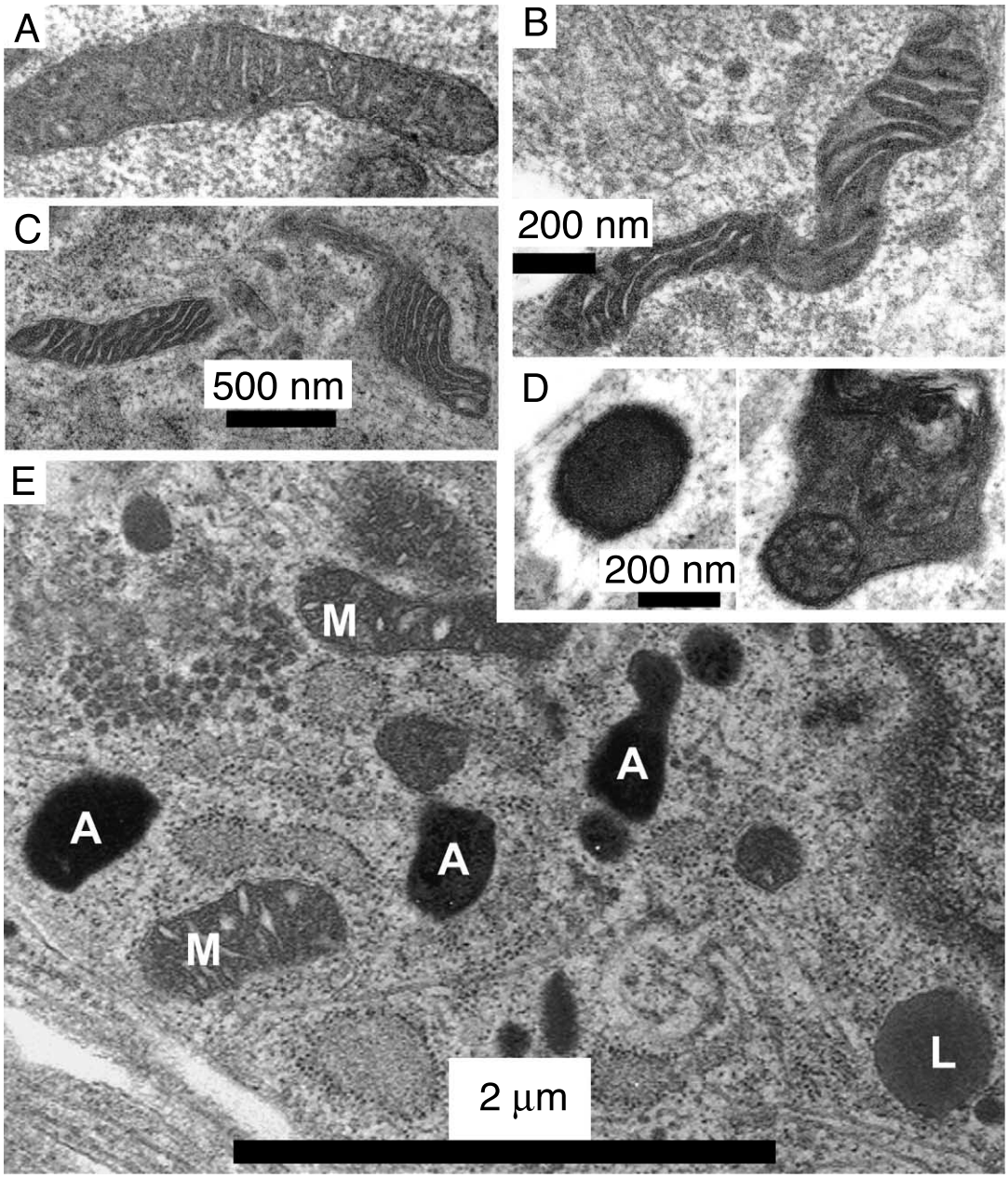

Fig. 8. Electron micrographs showing mitochondria and other organelles in neurons deprived of NGF for 30 h and maintained in medium containing: (A) CHX (1 µg/ml), (B) L-NAC (30 mM), (C) BAF (30 µM), (D–E) deprivation alone. Note that mitochondria in cells maintained by CHX, L-NAC, and BAF appear similar to those in cells deprived for the same time without the compounds (Fig. 6). Scale in (A) and (B) is the same. (D) Examples of a lysosome (left) and an autophagosome (right) in neurons deprived of NGF for 30 h. Note the organelles engulfed by the autophagosome. Lysosomes were recognized on micrographs as the most electron-dense bodies in the cytoplasm of cells. At high magnifications a faint bounding membrane was also apparent. Autophagosomes were recognized in micrographs as membrane-bound organelles with other organelles clearly contained within them. (E) Micrograph of a cell deprived of NGF for 30 h. M, mitochondria; A, lysosome (A = autophagic particle); L, lipid droplet.

cytoplasmic area occupied by mitochondrial profiles was the same even though cell volume had decreased, the implication is that mitochondrial volume per unit area of cytoplasm was similar to that in control. This was only possible if mitochondria were lost from cells but the loss was masked by concurrent cellular shrinkage that concentrated the remaining mitochondria into a smaller area. Thus, it appears that the total mitochondrial mass per cell had declined by 24 h after NGF deprivation. However, all NGF-deprived neurons inspected ($n = 63$; 24–30 h withdrawal) had numerous mitochondrial profiles. Therefore, the loss of NAO staining could not be explained by a loss of mitochondria. Because a large portion of cells did not stain for NAO by 24–30 h after NGF withdrawal (Figs. 1, 2), this finding suggests that cardiolipin was lost from mitochondria

before there were any obvious changes in mitochondrial morphology.

Mitochondrial loss was inhibited by CHX, L-NAC, and BAF

Figure 8A, B, C shows electron micrographs of mitochondria in neurons deprived of NGF for 30 h and maintained in a viable state with culture medium containing BAF, CHX, or L-NAC. The morphology of these mitochondria appeared indistinguishable from that of mitochondria in cells deprived of NGF for the same period without these compounds. Morphometric analysis of electron micrographs revealed that the average cross-sectional area of a mitochondrion in NGF-deprived neurons maintained in CHX or L-NAC decreased by more than the average cross-sectional area of a mitochondrion in NGF-deprived neurons not exposed to these compounds (Fig. 7C; $P < 0.001$). However, treatment of NGF-deprived cells with BAF prevented mitochondrial shrinkage. Indeed, the average cross-sectional area of a mitochondrion in cells deprived of NGF and maintained in BAF for 30 h was not significantly different from that of a mitochondrion in control cells ($P > 0.1$). The average cross-sectional area of a mitochondrion in BAF-saved cells remained unchanged for at least 3 days after NGF deprivation (not shown). The average cross-sectional area of the cytoplasm occupied by mitochondria of cells deprived of NGF for 30 h and exposed to BAF, CHX, or L-NAC was significantly higher than that of cells deprived of NGF for the same period without the compounds (Fig. 7D; $P < 0.001$ in each case). There were two possible explanations for this finding: (1) the treatments caused an increase in total cellular mitochondrial volume or (2) loss of mitochondrial mass in NGF-deprived cells was prevented by the treatments. By 3 days after NGF deprivation, there was a decline in the total cytoplasmic area occupied by mitochondria in cells maintained in BAF-containing medium so that the occupied area was not significantly different from that found in control cells ($6.8 \pm 0.7\%$ of total; $P > 0.5$). This decrease may have been caused by a slow loss of mitochondria in these cells similar to that reported for freshly-plated sympathetic neurons deprived of NGF and maintained in BAF (Xue et al., 1999).

To further investigate changes in mitochondrial mass after NGF deprivation, we determined the content of the mitochondrial matrix heat-shock protein, Hsp60, in NGF-maintained and -deprived cultures. Western blot analysis showed that there was a significant loss of Hsp60 content in cultures deprived of NGF for 24–30 h ($P < 0.01$; Fig. 7E). The Hsp60 content of cultures deprived of NGF for 30 h and maintained in culture medium containing BAF, CHX, or L-NAC was not significantly different from that of control cultures maintained in the presence of NGF (Fig. 7F; $P > 0.05$ in each case) suggesting that these compounds did not cause proliferation of mitochondria but, rather, prevented changes of mitochondrial volume. Taken together, the data suggest that there was an actual decrease of mitochondrial volume after NGF deprivation and that this decrease was masked in electron micrographs of these cells by atrophic 'concentration' of mitochondria. Additionally, they suggest that the apparent increase in mitochondrial volume in micrographs of NGF-deprived cells maintained in BAF-, CHX-, or L-NAC-containing media was illusory as it was caused by preservation of mitochondria in cells undergoing atrophy rather than by mitochondrial proliferation.

Table 2. Effects of BAF, CHX, and L-NAC on formation of lysosomes and autophagosomes after NGF withdrawal

Conditions	Average # of lysosomes and autophagosomes/10 μm^2 of cytoplasm
+NGF	0.59 ± 0.20 (39)
−NGF (24 h)	2.07 ± 0.40 (28)*
−NGF (30 h)	3.22 ± 1.20 (30)*
−NGF, BAF (30 h, 30 μM)	0.78 ± 0.24 (26)
−NGF, CHX (30 h, 1 μg/ml)	0.65 ± 0.39 (29)
−NGF, L-NAC (30 h, 30 mM)	0.88 ± 0.35 (26)

Data were taken from transmission electron micrographs (from two to three separate platings). Lysosomes and autophagosomes were identified as shown in Fig. 8D, E and as described by Xue et al. (1999). Only those profiles that could be unambiguously identified as being lysosomal/autophagic were counted. Numbers in parentheses are the number of different cellular profiles inspected. Asterisks indicate significantly ($P < 0.02$) different from cells maintained in the presence of NGF.

Mitochondria were probably degraded via an autophagic pathway

Xue et al. (1999) showed that there is an increase in autophagosomes (Klionsky and Emr, 2000) in NGF-deprived sympathetic neurons and presented evidence consistent with a role for autophagy in the apoptotic death of these cells. Because autophagy is the primary pathway for degradation of intracellular organelles, including mitochondria (Lemasters et al., 1998; Fletcher et al., 2000; Klionsky and Emr, 2000), it seemed likely to us that the decrease of mitochondrial mass in NGF-deprived neurons was caused by elimination of mitochondria by an autophagic process. Consistent with this hypothesis, we observed increased numbers of lysosomes and autophagosomes in electron micrographs of NGF-deprived neurons (Figs. 6E, 8D, E). Table 2 shows that this increase was significant. Lysosome and autophagosome proliferation was inhibited by BAF, CHX, and L-NAC suggesting a role for ROS and caspases in their formation. The most parsimonious explanation for these findings is that there was ROS-induced damage to mitochondria during apoptotic death, that this damage was at least partially caused by increased ROS, and that the damaged mitochondria were then eliminated by autophagy.

DISCUSSION

We conducted a study of changes in cellular cardiolipin content and mitochondrial mass during the programmed death of NGF-deprived rat sympathetic

neurons in cell culture. By 24 h after NGF withdrawal, only about 70% of these cells stained with the cardiolipin-specific dye, NAO. By 2 days after withdrawal, almost none of the cellular debris remaining in the culture dish stained with this dye. The loss of NAO staining suggested extensive degradation of cardiolipin in dying neurons. Gas chromatographic measurements of cardiolipin, phosphatidylethanolamine, and phosphatidylcholine concentrations showed that there was an extensive loss of all three lipids after NGF deprivation. Approximately the same amount of phosphatidylethanolamine and phosphatidylcholine was lost from cultures after NGF withdrawal. The loss of cardiolipin in deprived cultures was greater than the loss of either of these lipids, confirming that this important mitochondrial IM lipid (Paradies et al., 1997) was selectively lost from cells during the apoptotic process. The global loss of lipids in NGF-deprived cultures appears to have been caused, in part, by decreased lipid synthesis without a concurrent suppression in the rate of lipid degradation. The loss could not be explained by increased lipid degradation because there was no significant increase in degradation after NGF deprivation.

Redistribution of cytochrome *c* from the mitochondria of rat sympathetic neurons in culture into the cytoplasm begins 12–18 h after NGF deprivation. The rate of cytochrome *c* release reaches a peak by 24 h after withdrawal, a time when ~50% of cells are committed to apoptotic death (Deckwerth and Johnson, 1993). Accompanying cytochrome *c* release in NGF-deprived cells is an increase of mitochondrial-derived ROS (Kirkland and Franklin, 2001). The period when cardiolipin was lost from mitochondria of NGF-deprived neurons, therefore, corresponded with the period of cytochrome *c* release and of increased ROS production. Because cardiolipin is unsaturated and is located in the mitochondrial IM, the source of ROS, it is highly susceptible to destruction by lipid peroxidation (Hockenbery et al., 1993; Polyak et al., 1997). This suggested to us that at least one mechanism for the cardiolipin loss after NGF deprivation was ROS-induced lipid peroxidation. Cells that had incorporated the oxidation-sensitive fluorescent fatty acid, *cis*-parinaric acid into their membranes lost fluorescence concurrently with the rise in ROS levels caused by NGF deprivation (Kirkland and Franklin, 2001) indicating that lipid peroxidation did, indeed, occur after NGF withdrawal. Both CHX and L-NAC, which inhibit accumulation of ROS in NGF-deprived cells by up-regulating cellular glutathione concentration (Kirkland and Franklin, 2001), completely blocked the reduction in *cis*-parinaric fluorescence after NGF deprivation. The broad-spectrum caspase inhibitor, BAF, which greatly attenuates the ROS burst (Kirkland and Franklin, 2001), also blocked the loss of *cis*-parinaric fluorescence after NGF withdrawal. Consistent with ROS/peroxidation-mediated loss of cardiolipin, CHX, L-NAC, and BAF also inhibited loss of NAO staining after NGF deprivation. Also consistent with a role for ROS in loss of cardiolipin we have found that deletion of the proapoptotic protein, Bax, from mouse sympathetic neurons blocks the ROS burst caused by NGF withdrawal and also blocks loss of NAO staining (unpublished results).

A principal hypothesis for how cytochrome *c* exits mitochondria during apoptosis is that the permeability transition pore in the mitochondrial IM opens, causing mitochondrial swelling and rupture of the mitochondrial OM (Szabó and Zoratti, 1991, 1992; Von Ahsen et al., 2000). However, Martinou et al. (1999) reported that mitochondria do not swell, but rather shrink in NGF-deprived sympathetic neurons during the time of cytochrome *c* redistribution and that there is no evidence of OM rupture. Furthermore, they found that in cells saved from death by a caspase inhibitor mitochondria were well preserved and could be replenished with cytochrome *c* upon re-exposure to NGF. We repeated and extended these findings using transmission EM. Electron micrographs revealed little morphological alteration of mitochondria 24 h after NGF deprivation, the peak period for cytochrome *c* release and ROS production (Kirkland and Franklin, 2001). Consistent with the findings of Martinou et al. (1999), we found that mitochondria were slightly smaller in cells deprived of NGF for 24 h than in control cells but that otherwise they appeared similar to those in NGF-maintained cells. No swollen mitochondria were observed in any neurons deprived of NGF for 24 or 30 h. Therefore, rupture of the mitochondrial OM secondary to swelling cannot explain cytochrome *c* release in these cells. Few mitochondria were visible in their entirety because they were not completely contained within single EM sections. Therefore, it was not possible to determine whether the OM extended completely without interruption around individual mitochondria. BAF inhibited loss of cardiolipin in NGF-deprived neurons but does not affect the rate of cytochrome *c* release in them (see Kirkland and Franklin, 2001). Therefore, it is unlikely that cardiolipin degradation caused cytochrome *c* redistribution. A more likely scenario is that caspases activated by cytochrome *c* release augmented mitochondrial ROS production and these ROS then caused the cardiolipin loss.

Total mitochondrial mass had declined in neurons deprived of NGF for 24 h. However, because NGF withdrawal also causes profound atrophy in these cells (Franklin and Johnson, 1998) the total mitochondrial volume on a per cell basis remained relatively constant. All cells at this stage had mitochondria. In NGF-deprived cells treated for 30 h with CHX, L-NAC, or BAF, mitochondrial mass was preserved. Xue et al. (1999) recently demonstrated that freshly dissociated rat sympathetic neurons deprived of NGF have an increased number of autophagosomes and suggested that autophagy is involved in the death process. We also noted increased numbers of lysosomes and autophagosomes in NGF-deprived sympathetic neurons that had been in culture for about a week. Because mitochondria turnover occurs primarily via an autophagic pathway (Lemasters et al., 1998; Klionsky and Emr, 2000) it seems likely that the loss of mitochondrial mass after NGF deprivation was caused by autophagocytosis of damaged mitochondria. Consistent with this hypothesis, we found that CHX, BAF, and L-NAC blocked the

elevation in lysosome and autophagosome numbers. Treatment of NGF-deprived cells with BAF prevented increased numbers of lysosomes and autophagosomes for at least 30 h after NGF deprivation. This finding contrasts with that of Xue et al. (1999) who reported that BAF causes only partial suppression of lysosome and autophagosome formation in these cells after a 14–16 h period of NGF withdrawal. The difference in the two sets of data likely results from dissimilar death paradigms. Xue et al. plated freshly dissociated cells without NGF while we withdrew NGF from neurons that had been established in culture for 6–9 days. Because freshly-plated, NGF-deprived sympathetic neurons die much more quickly than do established cultures (Edwards and Tolkovsky, 1994), the differences in the degree of BAF effect on formation of autophagosomes in the two death paradigms likely reflect differences in rate of autophagy associated with death. Based on the findings reported here we propose that the ROS burst damages cardiolipin in the mitochondrial IM and, perhaps, other mitochondrial constituents and that this damage then leads to mitochondrial destruction via an autophagic pathway (Fletcher and Emr, 2000; Klionsky et al., 2000).

CONCLUSION

We demonstrated that cardiolipin is lost from the IM of mitochondria in NGF-deprived sympathetic neurons before there are any obvious changes in mitochondrial morphology. The most likely cause for this loss was lipid peroxidation induced by an increase in production of free radical oxygen by mitochondria. Total mitochondrial mass declined after NGF deprivation. This decline was, at least temporarily, blocked by agents that have antioxidant effects. There is considerable evidence supporting a role for reactive oxygen in the apoptotic death of many cell types (Hockenbery et al., 1993; Kane et al., 1993; Tan et al., 1998; Kirkland and Franklin, 2001). The data presented here provide evidence that one of the deleterious effects of reactive oxygen during apoptosis is mitochondrial damage and destruction.

Acknowledgements—This work was supported by a grant to the University of Wisconsin Medical School under the Howard Hughes Medical Institute Research Resources Program for Medical Schools and by National Institutes of Health grant NS37110.

REFERENCES

Deckwerth, T.L., Johnson, E.M., Jr., 1993. Temporal analysis of events associated with programmed cell death (apoptosis) of sympathetic neurons deprived of nerve growth factor. J. Cell Biol. 123, 1207–1222.

Deshmukh, M., Johnson, E.M., Jr., 1998. Evidence of a novel event during neuronal death: development of competence-to-die in response to cytoplasmic cytochrome c. Neuron 21, 695–705.

Deshmukh, M., Vasilakos, J., Deckwerth, T.L., Lampe, P.A., Shivers, B.D., Johnson, E.M., Jr., 1996. Genetic and metabolic status of NGF-deprived sympathetic neurons saved by an inhibitor of ICE-family proteases. J. Cell Biol. 135, 1341–1354.

Dugan, L.L., Creedon, D.J., Johnson, E.M., Jr., Holtzman, D.M., 1997. Rapid suppression of free radical formation by nerve growth factor involves the mitogen-activated protein kinase pathway. Proc. Natl. Acad. Sci. USA 94, 4086–4091.

Edwards, S.N., Tolkovsky, A.M., 1994. Characterization of apoptosis in cultured rat sympathetic neurons after nerve growth factor withdrawal. J. Cell Biol. 124, 537–546.

Fletcher, G.C., Xue, L., Passingham, S.K., Tolkovsky, A.M., 2000. Death commitment point is advanced by axotomy in sympathetic neurons. J. Cell Biol. 150, 741–754.

Franklin, J.L., Johnson, E.M., Jr., 1998. Control of neuronal size homeostasis by trophic factor-mediated coupling of protein degradation to protein synthesis. J. Cell Biol. 142, 1313–1324.

Franklin, J.L., Sanz-Rodriguez, C., Juhasz, A., Deckwerth, T.L., Johnson, E.M., Jr., 1995. Chronic depolarization prevents programmed death of sympathetic neurons *in vitro* but does not support growth: Requirement for Ca^{2+} influx but not Trk activation. J. Neurosci. 15, 643–664.

Greenlund, L.J.S., Deckwerth, T.L., Johnson, E.M., Jr., 1995. Superoxide dismutase delays neuronal apoptosis: a role for reactive oxygen species in programmed neuronal death. Neuron 14, 303–315.

Halliwell, B., Gutteridge, J.M.C., 2000. Free Radicals in Biology and Medicine, 3rd edn. Clarendon Press, Oxford, pp. 407–411.

Hockenbery, D.M., Oltvai, Z.N., Yin, X-M., Millman, C.L., Korsmeyer, S.J., 1993. Bcl-2 functions in an antioxidant pathway to prevent apoptosis. Cell 75, 241–251.

Johnson, M.I., Argiro, V., 1983. Techniques in the tissue culture of rat sympathetic neurons. Methods Enzymol. 103, 334–347.

Kane, D.J., Sarafian, T.A., Anton, R., Hahn, H., Gralla, E.B., Valentine, J.S., Örd, T., Bredesen, D.E., 1993. Bcl-2 inhibition of neural death: decreased generation of reactive oxygen species. Science 262, 1274–1277.

Keij, J.F., Bell-Prince, C., Steinkamp, J.A., 2000. Staining of mitochondrial membranes with 10-nonyl acridine orange MitoFluor Green, and MitoTracker Green is affected by mitochondrial membrane potential altering drugs. Cytometry 39, 203–210.

Kirkland, R.A., Franklin, J.L., 2001. Evidence for redox regulation of cytochrome c release in programmed neuronal death: antioxidant effects of protein synthesis and caspase inhibition. J. Neurosci. 21, 1949–1963.

Klionsky, D.J., Emr, S.D., 2000. Autophagy is a regulated pathway of cellular degradation. Science 290, 1717–1721.

Kluck, R.M., Bossy-Wetzel, E., Green, D.R., Newmeyer, D.D., 1997. The release of cytochrome c from mitochondria: a primary site for Bcl-2 regulation of apoptosis. Science 275, 1132–1136.

Lemasters, J.J., Nieminen, A.L., Qian, T., Trost, L.C., Elmore, S.P., Nishimura, Y., Crowe, R.A., Cascio, W.E., Bradham, C.A., Brenner, D.A., Herman, B., 1998. The mitochondrial permeability transition in cell death: a common mechanism in necrosis, apoptosis and autophagy. Biochim. Biophys. Acta 1366, 177–196.

Li, P., Nijhawan, D., Budihardjo, I., Srinivasula, S.M., Ahmad, M., Alnemri, E.S., Wang, X., 1997. Cytochrome c and dATP-dependent formation of Apaf-1/caspase-9 complex initiates an apoptotic protease cascade. Cell 91, 479–489.

Martin, D.P., Schmidt, R.E., DiStefano, P.S., Lowry, O.H., Carter, J.G., Johnson, E.M., Jr., 1988. Inhibitors of protein synthesis and RNA synthesis prevent neuronal death caused by nerve growth factor deprivation. J. Cell Biol. 106, 829–844.

Martinou, I., Desagher, S., Eskes, R., Antonsson, B., André, E., Fakan, S., Martinou, J.C., 1999. The release of cytochrome c from mitochondria during apoptosis of NGF-deprived sympathetic neurons is a reversible event. J. Cell Biol. 144, 883–889.

Neame, S.J., Rubin, L.L., Philpott, K.L., 1998. Blocking cytochrome c activity within intact neurons inhibits apoptosis. J. Cell Biol. 142, 1583–1593.

Oppenheim, R.W., 1991. Cell death during development of the nervous system. Annu. Rev. Neurosci. 14, 453–501.
Paradies, G., Petrosillo, G., Ruggiero, F.M., 1997. Cardiolipin-dependent decrease of cytochrome c oxidase activity in heart mitochondria from hyperthyroid rats. Biochim. Biophys. Acta 1319, 5–8.
Petit, J., Huet, O., Gallet, P.F., Maftah, A., Ratinaud, M., Julien, R., 1994. Direct analysis and significance of cardiolipin transverse distribution in mitochondrial inner membranes. Eur. J. Biochem. 220, 871–879.
Petit, J.M., Maftah, A., Ratinaud, M.H., Julien, R., 1992. 10N-nonyl acridine orange interacts with cardiolipin and allows the quantitation of this phospholipid in isolated mitochondria. Eur. J. Biochem. 209, 267–273.
Pettman, B., Henderson, C.E., 1998. Neuronal cell death. Neuron 20, 633–647.
Polyak, K., Xia, Y., Zweier, J.L., Kinzler, K.W., Vogelstein, B., 1997. A model for p53-induced apoptosis. Nature 389, 300–305.
Poot, M., Pierce, R.H., 1999. Detection of changes in mitochondrial function during apoptosis by simultaneous staining with multiple fluorescent dyes and correlated multiparameter flow cytometry. Cytometry 35, 311–317.
Rao, A.M., Hatcher, J.F., Dempsey, R.J., 2000. Lipid alterations in transient forebrain ischemia: possible new mechanisms of CDP-choline neuroprotection. J. Neurochem. 75, 2528–2535.
Rao, A.M., Hatcher, J.F., Dempsey, R.J., 2001. Does CDP-choline modulate phospholipase activities after transient forebrain ischemia? Brain Res. 893, 268–272.
Ratan, R.R., Murphy, T.H., Baraban, J.M., 1994. Macromolecular synthesis inhibitors prevent oxidative stress-induced apoptosis in embryonic cortical neurons by shunting cysteine from protein synthesis to glutathione. J. Neurosci. 14, 4385–4392.
Reed, J.C., 1997. Cytochrome c: can't live with it–can't live without it. Cell 91, 559–562.
Szabó, I., Zoratti, M., 1991. The giant channel of the inner mitochondrial membrane is inhibited by cyclosporin A. J. Biol. Chem. 266, 3376–3379.
Szabó, I., Zoratti, M., 1992. The mitochondrial megachannel is the permeability transition pore. J. Bioenerg. Biomembr. 24, 111–117.
Tan, S., Sagara, Y., Liu, Y., Maher, P., Schubert, D., 1998. The regulation of reactive oxygen species production during programmed cell death. J. Cell Biol. 141, 1423–1432.
Von Ahsen, O., Waterhouse, N.J., Kuwana, T., Newmeyer, D.D., Green, D.R., 2000. The 'harmless' release of cytochrome c. Cell Death Diff. 7, 1192–1199.
Xue, L., Fletcher, G.C., Tolkovsky, A.M., 1999. Autophagy is activated by apoptotic signaling in sympathetic neurons: an alternative mechanism of death execution. Mol. Cell. Neurosci. 14, 180–198.
Zou, H., Henzel, W.J., Liu, X., Lutschg, A., Wang, X., 1997. Apaf-1, a human protein homologous to *C. elegans* CED-4, participates in cytochrome c-dependent activation of caspase-3. Cell 90, 405–413.

(*Accepted* 28 *May* 2002)